Estuarine, Coastal and Shelf Science 203 (2018) 17–28

Contents lists available at ScienceDirect

Estuarine, Coastal and Shelf Science

journal homepage: www.elsevier.com/locate/ecss

Nutrient input through submarine groundwater discharge in two major Chinese estuaries: the Pearl River Estuary and the Changjiang River Estuary

Jianan Liu [a], Jinzhou Du [a, *], Ying Wu [a], Sumei Liu [b]

[a] State Key Laboratory of Estuarine and Coastal Research, East China Normal University, Shanghai, 200062, China
[b] Key Laboratory of Marine Chemistry Theory and Technology, Ministry of Education, Ocean University of China/ Laboratory for Marine Ecology and Environmental Science, Qingdao National Laboratory for Marine Science and Technology, Qingdao, 266100, China

ARTICLE INFO

Article history:
Received 1 September 2017
Received in revised form
26 January 2018
Accepted 1 February 2018
Available online 5 February 2018

Keywords:
Submarine groundwater discharge
Radium isotopes
Nutrient fluxes
Pearl River Estuary
Changjiang River Estuary

ABSTRACT

In this study, we used a ^{224}Ra mass balance model to evaluate the importance of submarine groundwater discharge (SGD) for the budgets of biogenic elements in two major Chinese estuaries: the Pearl River Estuary (PRE) and the Changjiang River Estuary (CRE). The apparent water age in the PRE was estimated to be 4.8 ± 1.1 days in the dry season and 1.8 ± 0.6 days in the wet season using a physical model based on the tidal prism. In the dry season, the water age in the CRE was estimated to be 11.7 ± 3.0 days using the ^{224}Ra/^{223}Ra activities ratios apparent age model. By applying the ^{224}Ra mass balance model, we obtained calculations of the SGD flow in the PRE of (4.5–10) × 10^8 m^3 d^{-1} (0.23–0.50 m^3 m^{-2} d^{-1}) and (1.2–2.7) × 10^8 m^3 d^{-1} (0.06–0.14 m^3 m^{-2} d^{-1}) in the dry season and wet season, respectively, and the estimated SGD flux was (4.6–11) × 10^9 m^3 d^{-1} (0.18–0.45 m^3 m^{-2} d^{-1}) in the dry season of the CRE. In comparison with the nutrient fluxes from the rivers, the SGD-derived nutrient fluxes may play a vital role in controlling the nutrient budgets and stoichiometry in the study areas. The large amount of dissolved inorganic nitrogen and phosphorus fluxes together with high N: P ratios into the PRE and CRE would potentially contribute to eutrophication and the occurrence of red tides along the adjacent waters.

1. Introduction

A river-dominated estuary and the adjacent sea are important regions where the continuous exchange of water and chemical components occurs between land/ocean interaction zones; therefore, these areas play a major role in terms of global biogeochemical cycles (e.g., Rengarajan and Sarma, 2015). In the past two decades, submarine groundwater discharge (SGD), which defined as the flow of water from the seabed to the ocean along continental margins, with scales lengths of meters to kilometers, regardless of fluid composition or driving force (Burnett et al., 2003; Moore, 2010), it has been shown to not only be an important component of the hydrological cycle (Moore et al., 2008) but also delivers a large amount of nutrients (e.g., Moore et al., 2006), trace elements (e.g., Beck et al., 2007a), radionuclides (e.g., Garcia-Orellana et al., 2013) and organic and inorganic carbon (e.g., Kim et al., 2011; Liu et al., 2014) to the oceans due to the biological and chemical reactions at the interface between the freshwater in the aquifer and the salt-water front. The large amount of nutrient input to the coastal zone, in particular, the high N: P ratios provided by the SGD, has the potential to impact the chemical budgets of water ecosystems through changing the nutrient ratios, which may cause eutrophication (e.g., Hwang et al., 2005a), harmful algal blooms (e.g., Hwang et al., 2005b) and hypoxia (e.g., McCoy et al., 2011). For example, Lee et al. (2009) suggested that the large and continuous supply of nutrient through SGD plays a significant role in the occurrence of eutrophication and red tides in the Masan Bay, Korea. Recently, an increasing number of studies have shown that SGD may be one of the important pathways for terrigenous materials entering the estuaries, so the SGD in estuaries deserves further attention and should be the focus of future investigations (e.g., Kolker et al., 2013; Rengarajan and Sarma, 2015).

In the previous SGD studies, the application of naturally occurring geochemical tracers has been shown to successfully enable integrated estimations of SGD over a range of spatial and temporal scales (e.g., Garcia-Orellana et al., 2014; Moore et al., 2006). Among

* Corresponding author.
E-mail address: jzdu@sklec.ecnu.edu.cn (J. Du).

https://doi.org/10.1016/j.ecss.2018.02.005
0272-7714/

these, the radium (Ra) quartet of isotopes (^{224}Ra, ^{223}Ra, ^{228}Ra, and ^{226}Ra) are known as powerful tools widely used to assess the flux sources and evaluate SGD into the coastal waters (e.g., Beck et al., 2007b; Moore, 1996, 2003), and the Ra-based SGD estimation generally represents the average level across the study region rather than a value in a single location within the study region.

The Pearl River (Zhujiang) Estuary (PRE) and Changjiang (Yangtze) River Estuary (CRE), as two largest estuaries in China in terms of freshwater discharge, are located in subtropical and temperate region, respectively. In recent decades, anthropogenic activities (i.e., agriculture, land-consuming changes and dam structures) have caused considerable changes in the riverine materials fluxes to the PRE and CRE and their adjacent sea areas (e.g., He et al., 2010; Li et al., 2007; Zhang et al., 1999). In our previous work, we reported that the SGD flux into the CRE was 6–30% of the Changjiang River discharge at the flood stage, showing the importance of SGD in hydrology; however, there were no nutrient fluxes reported from the SGD (Gu et al., 2012). Also in the PRE, the significance of SGD and SGD-derived nutrients to the estuarine waters are still unknown. Because of the relatively short water ages in the PRE and CRE (Sun et al., 2014; Xu et al., 2013), the short half-lives isotopes of ^{223}Ra ($T_{1/2} = 11.4$ days) and ^{224}Ra ($T_{1/2} = 3.66$ days) could be applicable for accurately estimating the SGD in such short time scales. Therefore, in this study, we developed a ^{224}Ra mass balance model to estimate the seasonal magnitude of SGD fluxes in both the PRE and CRE, which are different types of estuaries. Moreover, a comparison study was also conducted to determine the quantities of SGD-derived nutrient and to evaluate its effluence in the PRE and CRE.

2. Study areas

The PRE and the CRE are two typical, largest estuaries in China. The PRE is located in the southern coast of China, along the northern boundary of the South China Sea, and it receives a large freshwater discharge of ~1.7×10^{11} m^3 yr^{-1} from the Pearl River that includes the East River, North River and West River (Fig. 1a). The PRE has a narrow head of only ~5 km at the upper estuary and a relatively wide sea entrance of ~60 km at the southern end, with an average depth of ~6 m and surface area of 2000 km^2, respectively (Sun et al., 2014). The tide in the PRE mainly flows from the Pacific oceanic tidal propagation through the Luzon strait, with amplitudes typically varying from 1 m to 1.8 m within the estuary (Mao et al., 2004; Cai et al., 2014).

The Changjiang River is the largest river in China and is the fifth largest river in the world that empties into the East China Sea. The freshwater discharge is ~8.7×10^{11} m^3 yr^{-1}, and the sediment load sharply decreased to ~0.15×10^9 tons yr^{-1} in 2010s, following the construction of the Three Gorges Dam (Dai and Lu, 2014). The study site of the CRE and its adjacent sea is located in the east coastal area of Eastern China, ends at a longitude of 123.5 °E and a latitude between 29.5 °N and 32 °N. The study area has an estimated area of ~2.5×10^4 km^2, which covers the Jiangsu southeast zone, the Shanghai sea, Hangzhou Bay and the Zhoushan waters (Fig. 1c). The inner estuary of the CRE is a meso-tidal estuary with average tides ranging from 2.4 m to 3.2 m (Yan et al., 2011).

The PRE and CRE are highly sensitive to the subtropical and temperate monsoon climate, with an annual average precipitation of ~1830 mm and ~1160 mm, respectively (data from the China Meteorological Data Sharing Service System, http://cdc.nmic.cn/). It is clear that the dry season occurs from October to March, while the wet season occurs between April and September (Fig. 1b and d), and approximately 80% of freshwater discharge from the Pearl River and Changjiang River flows during the wet season. Due to the fast development of industrial/agricultural activities and urbanization in recent decades, anthropogenic activities could deplete the level of the groundwater in both the PRE and CRE (Du, 2006; Zhu et al., 2004). The acidified of groundwater, mainly caused by acid rain, has become a major environmental problem for groundwater (Jing et al., 2010). Furthermore, unreasonable exploitation and environmental pollution has led to a shortage of groundwater and groundwater quality deterioration in the PRE and CRE (Du, 2006; Zhu et al., 2004). In addition, the PRE and CRE have been receiving an increasing load of anthropogenic nutrients, especially the dissolved inorganic nitrogen and phosphorus (e.g., Huang et al., 2003; Harrison et al., 2008; Jiang et al., 2014; Li et al., 2007). These effects lead to eutrophication and seasonal hypoxia as major issues in the PRE and CRE, respectively (Huang et al., 2003; Liu et al., 2016), and extensive red tides also occur in both estuaries (Chen et al., 2007; Huang et al., 2003; Liu et al., 2013).

3. Sampling and methods

Ra isotopes samples in the PRE (Fig. 1a) were collected onboard the R/V *Nanfeng* during September 2014 (dry season) and June 2015 (wet season), and Ra isotopes samples in the CRE (Fig. 1c) were collected on board the R/V *Runjiang I* during March 2015 (dry season). All the Ra water samples (~60 L) were obtained from the surface water (at a depth of ~1 m) using a submerged pump. The seawater salinity and temperature were measured in situ using a Conductance-Temperature-Depth sensor. In addition, several groundwater (pore water, ~20 L, and well water, ~40 L) samples were collected as SGD end-members for the PRE and CRE; specifically, the respective groundwater samples were collected from the beaches and wells along the coast of Shengsi Island and Zhoushan in November 2014 and Chongming Island in April 2017 and the along the coast of the PRE in June 2016 (Fig. 1a and c).

The water samples for Ra isotopes were then run through columns filled with pre-weighed ~20 g Mn-coated acrylic fibers at a flow rate of ~0.5 L min^{-1} (Moore, 1976). After washing the Mn-fiber with Milli-Q water, the water content of the Mn-fiber was reduced to ~75% to obtain higher measurement efficient (Gu et al., 2012). ^{223}Ra and ^{224}Ra on the fiber were measured in the shipboard laboratory immediately after preparation, using a radium delayed coincidence counter (RaDeCC) (Moore and Arnold, 1996). The uncertainties of ^{223}Ra and ^{224}Ra were estimated to be approximately 20% and 5%, respectively, using the equations reported in Garcia-Solsona et al. (2008).

In groundwater, nutrient water samples were filtered with acid pre-cleaned 0.45 μm pore-size acetate cellulose filters, and then the filtrates were fixed with saturated $HgCl_2$ and stored in the dark. Upon return to the onshore laboratory, the nutrient samples were analyzed for dissolved inorganic nutrients (NO_2^-, NO_3^-, NH_4^+, PO_4^{3-} and $Si(OH)_4$) by an auto-analyzer (Model: Skalar SAN^{plus}) (Liu et al., 2005). The concentration of dissolved inorganic nitrogen (DIN) is expressed as the sum of NO_2^-, NO_3^-, and NH_4^+ concentrations.

4. Results

4.1. Hydrography

Geologically, the coast of PRE is mainly covered with Quaternary sediments, along with bedrock outcrops occupy in the southern regions of the PRE (Wang and Jiao, 2012). Groundwater aquifers in the watershed area of the PRE are unconsolidated deposits and bedrocks, which distribute in the northern and southern regions, respectively; while in the CRE, the coast type is alluvials and diluvials of accumulational plains in the northern regions and bedrocks in the southern regions (China hydrological geological map, 1984). The aquifers of unconsolidated deposits and

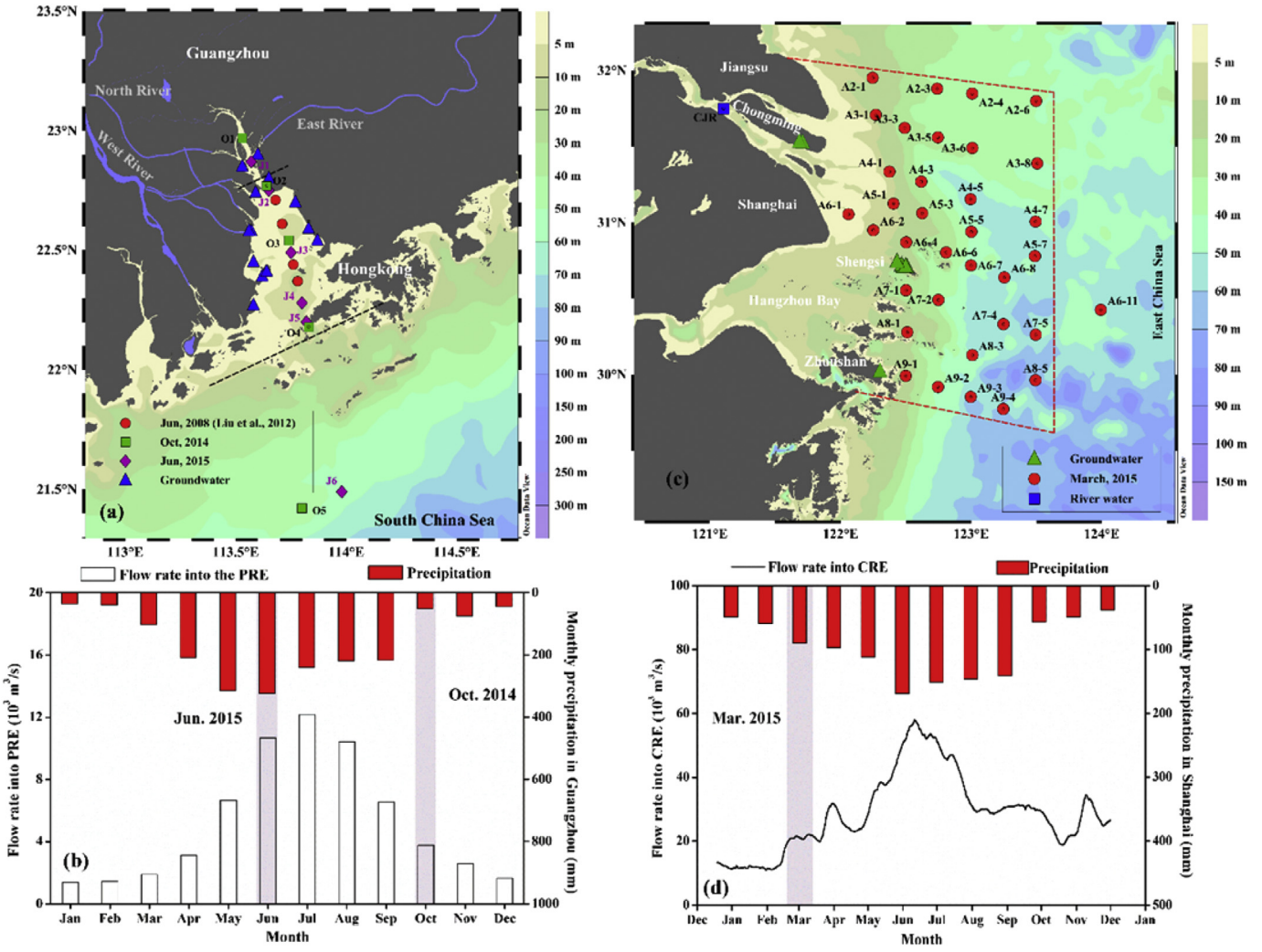

Fig. 1. A map of the study areas showing the sampling stations in the PRE(a) and CRE (c); (b) the river flow rate into the PRE (=flow rate of Xijiang/68.5% × 53% (Lu and Gan, 2015) and the monthly precipitation in Guangzhou. (d) Changjiang River water discharge into the CRE based on the Datong hydrographic station and the monthly precipitation in Shanghai; All the river discharge data are from the China Bureau of Hydrology, Ministry of Water Resources, http://xxfb.hydroinfo.gov.cn; all the precipitation data are from the China Meteorological Data Sharing Service System, http://cdc.nmic.cn/.

accumulational plains are usually developed with abundant water, while lower water content occurs in bedrocks. Overall, the groundwater in the PRE and CRE is not evenly distributed. Both the PRE and CRE are complex estuaries because of irregular topography, seasonally dynamic variations in freshwater discharge, monsoon winds and estuarine circulation. The coastal circulation governs the transports and distributions of physical and water quality parameters such as temperature and salinity. In this case, the hydrodynamic condition in the PRE and CRE are both very complicated.

In surface water of the PRE, the salinity increased from the estuary mouth to the open sea. Obviously, due to a smaller freshwater discharge from the Pearl River, the salinity was higher in the dry season (shown in the Supplementary Table). In the PRE, the water in vertical profile mixes well in both dry season and wet season because of the shallow water depth (Cai et al., 2004; Zhang et al., 2013). A similar salinity gradient was also observed in the CRE surface water, which salinity generally increased with offshore distance increasing (Fig. 2a). The CRE temperature in the dry season ranged from 9.4 to 14.1 °C which was much lower than that in the wet season (June) (Gu et al., 2012). Low temperature and high temperature anomalies occurred in the northwest and southeast of study area (Fig. 2b), respectively; these anomalies may due to the contribution of the Yellow Sea Coast Water and Taiwan Warm Water. From the density sigma-t (kg/m^3) distributions in vertical profile along the transect of central CRE (from stations A6-1 to A6-11, Fig. 3) we can see that in the upper layer, because of the Changjiang River freshwater discharge, a low density tongue was obviously observed from coast to offshore, and in the underlayer water, the upwelling signal from offshore to coast was apparent, especially in the 123°E area. In the east of 123°E there was no significant pycnocline observed, while in the west of 123 °E which was in the shallow regions near the coast, the pycnocline was observed.

4.2. Ra concentrations

Here, we describe the ^{224}Ra data as excess ^{224}Ra which are obtained by subtracting the ^{228}Th-supported ^{224}Ra from the total ^{224}Ra. All the ^{223}Ra and ^{224}Ra data in surface water of the PRE and CRE showed spatial and temporal variability in the study areas (shown in the Supplementary Table). In the PRE, the ^{224}Ra and ^{223}Ra activities in the dry season ranged from 129 dpm 100 L^{-1} to

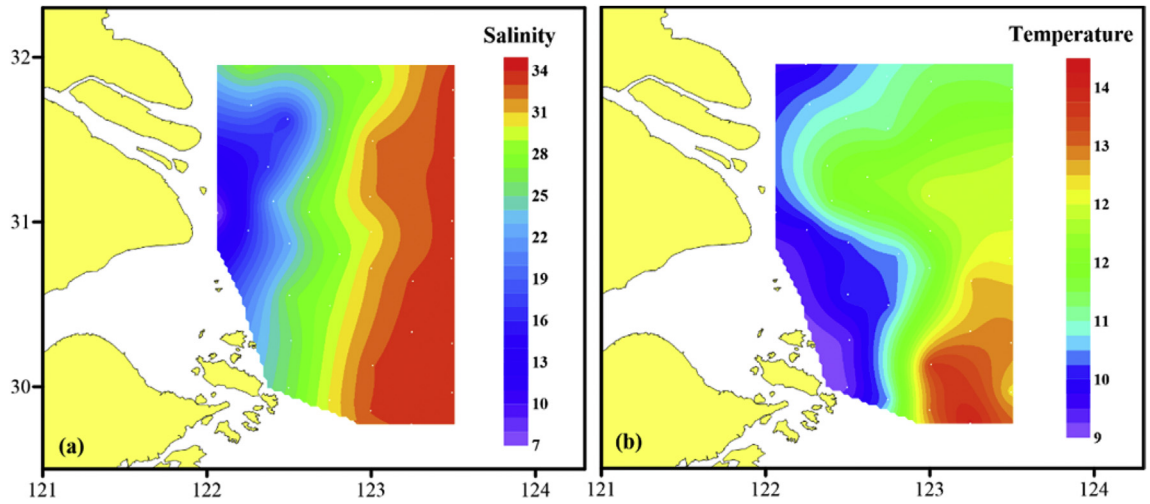

Fig. 2. Distributions of salinity and temperature in surface water of the CRE in March 2015 (color figure online).

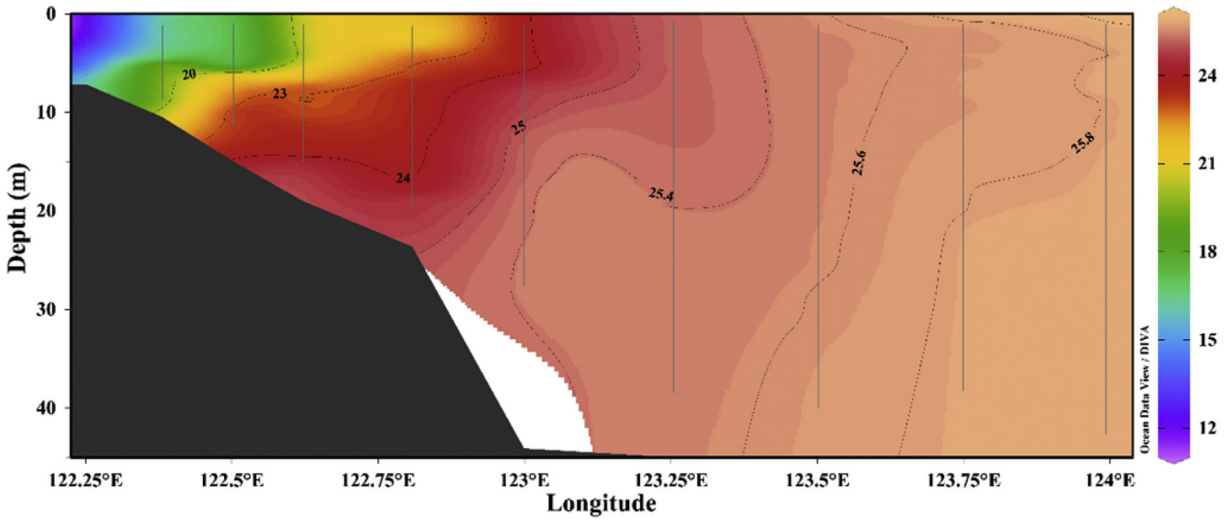

Fig. 3. Vertical distribution of density (sigma-t kg m^{-3}) along the transect from A6-1 to A6-11 during March 2015 (color figure online).

301 dpm 100 L^{-1} and from 4.5 dpm 100 L^{-1} to 13 dpm 100 L^{-1}, respectively. The Ra activities in the dry season were higher than those in the wet season, which the activities were ranged between 54 and 78 dpm 100 L^{-1} (^{224}Ra) and 1.7–4.0 dpm 100 L^{-1} (^{223}Ra). In the dry season of the CRE, ^{224}Ra and ^{223}Ra activities were varied from 1.3 dpm 100 L^{-1} to 161 dpm 100 L^{-1} and from almost undetectable (0 dpm 100 L^{-1}) to 7.9 dpm 100 L^{-1}, respectively. Similarly, ^{224}Ra and ^{223}Ra activities in the dry season were clearly higher than those in the wet season reported of 1.2–74.8 dpm 100 L^{-1} and 0.2 to 3.2 dpm 100 L^{-1} for ^{224}Ra and ^{223}Ra, respectively in our previous work (Gu et al., 2012). We can see that both ^{224}Ra and ^{223}Ra in the dry season have the higher activities, this could be more groundwater discharge with high Ra concentrated into the PRE and CRE in the dry season. In the broad CRE, the Ra activities were lower than those in the semi-closed and embedded PRE in the same season, and this may be determined by the dilution of the shelf water in the East China Sea water with low Ra activities.

Fig. 4 shows the scatter plots of the ^{224}Ra and ^{223}Ra activities versus salinity in surface water of the PRE and CRE. The distribution patterns in both the PRE and CRE were similar, with low activities at zero salinity, followed by Ra activities increased with salinity increasing, then the highest activities were reached at salinities of approximately 12–26; after the Ra activities peaked, they decreased to their lowest activities in high-salinity seawater. We can observe such similar coherent patterns in estuaries of other large rivers, which may reflect the release of ^{224}Ra and ^{223}Ra from particles into solution upon estuarine mixing (e.g., Moore and Krest, 2004; Rengarajan and Sarma, 2015; Xu et al., 2013). In the PRE, the ^{224}Ra/^{223}Ra ratios with the slope of fitting line were similar in the dry season and wet season, which were 23.8 ($r = 0.96$, $p < 0.001$) and 21.6 ($r = 0.75$, $p < 0.001$), respectively, indicating surface water in the PRE have similar sources (Fig. 5). As with the PRE, the relationship between ^{224}Ra and ^{223}Ra also showed similar ratios with a fitting line slope of 18.7 ($r = 0.79$, $p < 0.001$) in the CRE (Fig. 5).

In groundwater, Ra activities (dpm 100 L^{-1}) were in wide ranges of 4.7–34.8 (mean = 13.1 ± 2.6, average ± standard error (Stewart et al., 2015), same below) for ^{223}Ra and 242–1110 (mean = 485 ± 83.2) for ^{224}Ra in the PRE and 1.4–25.2 (mean = 10.2 ± 3.0) for ^{223}Ra and 11.3–898 (mean = 369 ± 113) for ^{224}Ra in the CRE, respectively (Supplementary Table). In both the PRE and CRE, Ra activities in most groundwater samples were much

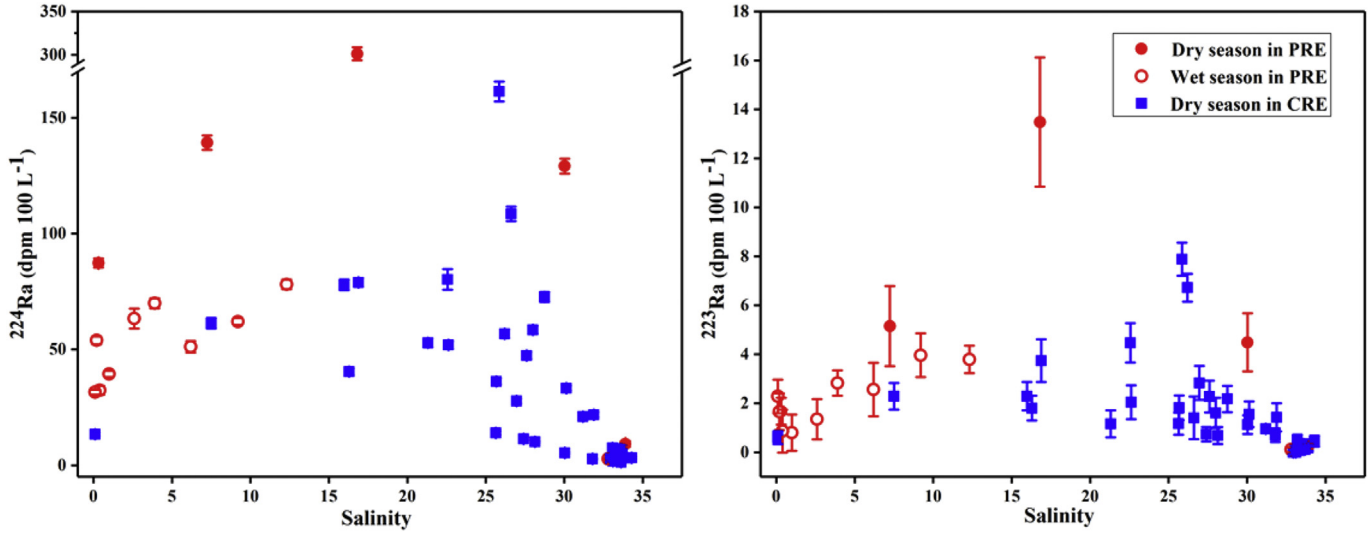

Fig. 4. Surface ^{224}Ra (a) and ^{223}Ra (b) activities (dpm 100 L^{-1}) versus salinity in the PRE and CRE. Data of wet season in the PRE includes four data cited from Liu et al. (2012).

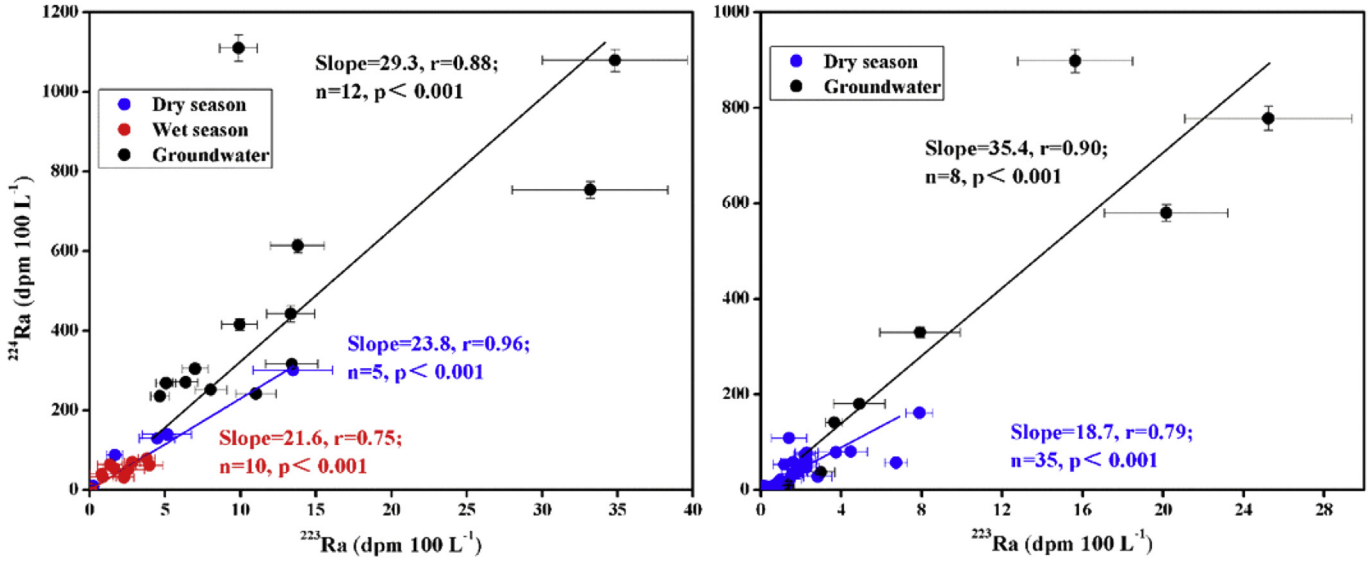

Fig. 5. Plots of ^{224}Ra vs. ^{223}Ra for all samples in the PRE and CRE (color figure online).

higher than those in surface water. Additionally, it is clearly seen that the linear fitting slopes of ^{224}Ra and ^{223}Ra in groundwater (slope = 29.3, r = 0.88 in the PRE and slope = 35.4, r = 0.90 in the CRE) are significant higher than the slope from the surface water, suggesting that the Ra input from groundwater may explain the Ra in surface water (Fig. 5).

5. Discussion

5.1. Water ages

Water age is defined as the time in a water parcel has spent since entering the estuary through its boundaries (Charette et al., 2008), and it can provide an available timescale for terrestrial material to accumulation in an estuary (Moore, 2000). Moreover, in order to estimate the fluxes of SGD into the PRE and CRE, the water ages of the estuaries must be known. Generally, there are two methods to access the water age in the study of SGD, which are Ra activity ratios and physical model. The PRE is a semi-enclosed estuary with the shape of an inverted funnel into the mainland and the main river input from the north, there are other Ra sources input from the tributaries in the west side of the estuary. Additionally, Ra diffusion from the bottom sediments to the surface water occurs due to the shallow depth of the PRE. Therefore, it is inappropriate to estimate the water age in the PRE by the ^{224}Ra/^{223}Ra ratio. However, the CRE has open water, and it is hard to calculate the tide prism from a physical model. Therefore, as described above, estimating the water age in the CRE by using the ^{224}Ra/^{223}Ra ratio method is feasible and a physical model will be used in the PRE.

5.1.1. Flushing time based on the physical model in the PRE

Following the assumptions of (1) the influence of the wind is negligible; (2) the PRE is well mixed, we use a physical model to estimate the flushing time in the PRE (Sanford et al., 1992; Moore et al., 2006):

$$T_f = \frac{V}{(1-b)P/T + I} \quad (1)$$

where T_f is the flushing time, V refers to the PRE volume, T is the tidal period, P is the tidal prism, b represents the return flow from the South China Sea into the PRE and I is the net inflow of Pearl River into the PRE during the sampling period. The value of b is equivalent to the fraction of open sea water, which can be obtained from the salinity in each measured sample dividing by the salinity in the open sea water. Because the surface area between the high and low tide was unknown, we calculated the tidal prism using Eqn. (2) which was determined by multiplying the average surface area by the tidal range during the sampling period in the PRE:

$$P = \int_H^0 A dz \quad (2)$$

where A is the average water surface area of the PRE, and z is the water depth over the tidal range (H).

Thus, with the parameters shown in Table 1, the average flushing time in the PRE by Eqn. (1) was estimated to be 4.8 ± 1.1 days and 1.8 ± 0.6 days in the dry season and wet season, respectively, which were comparable to the values which was reported as 6 days in the dry season and 3 days in the wet season (Sun et al., 2014). The flushing time in the PRE shows a predominant seasonal variation because of variance in the Pearl River discharge and tidal height.

5.1.2. Apparent age via Ra isotopes in the CRE

In the study area of the CRE, the average depth is ~34.7 m, and the Ra isotopes into surface water from bottom sediments can be neglected due to the relatively short time scale (Gu et al., 2012). Therefore, following Moore et al. (2006), assuming that the system is in a steady state, which the Ra additions are balanced by the losses, then the ^{224}Ra and ^{223}Ra balance in the CRE can be written as follows:

$$F^{224}Ra = I^{224}Ra(\lambda_{224} + 1/\tau) \quad (3)$$

$$F^{223}Ra = I^{223}Ra(\lambda_{223} + 1/\tau) \quad (4)$$

where $F^{224}Ra$ and $F^{223}Ra$ are the total ^{224}Ra and ^{223}Ra fluxes into the study system, $I^{224}Ra$ and $I^{223}Ra$ are the inventories of the ^{224}Ra and ^{223}Ra in the study system, and λ_{224} and λ_{223} are the decay constants for ^{224}Ra and ^{223}Ra, respectively. τ is the apparent age of water in the study system, which can be determined by dividing Eqn. (3) by Eqn. (4):

$$\tau = \frac{F\left[\frac{^{224}Ra}{^{223}Ra}\right] - I\left[\frac{^{224}Ra}{^{223}Ra}\right]}{\lambda_{224} I\left[\frac{^{224}Ra}{^{223}Ra}\right] - \lambda_{223} F\left[\frac{^{224}Ra}{^{223}Ra}\right]} \quad (5)$$

In general, the groundwater around the coast could be recognized as the input water. Therefore, in this study, we used the linear fitting slope between ^{224}Ra and ^{223}Ra in groundwater of 35.4 ± 4.0 as the initial input ratio in Eqn (5). Similarly, the linear fitting slope in surface water of 18.7 ± 1.6 was applied to as the ^{224}Ra and ^{223}Ra inventories in the CRE. The water age is thus determined to be 11.7 ± 3.0 days, which is comparable with that in May 2011 of 11.3 ± 5.2 days (Xu et al., 2013), but longer than that in the wet season in 2009 of 7.0 days (Gu et al., 2012), that may due to greater freshwater discharge of the Changjiang River in the wet season.

5.2. ^{224}Ra mass balance model

In a steady state system, a balance of Ra fluxes into the system and losses from the system is assumed (Moore et al., 2008). The ^{224}Ra inputs to the PRE and CRE include the dissolved and desorbable ^{224}Ra from rivers (I_{riv}), desorption from resuspended sediments (I_{res}), diffusion from bottom sediments (I_{diff}) and input associated with SGD (I_{SGD}). On the other hand, the ^{224}Ra output from the systems primarily by radioactive decay (L_{decay}) and mixing with low-^{224}Ra seawater (L_{mix}). The mass balance equation is built as follows:

$$I_{riv} + I_{res} + I_{diff} + I_{SGD} = L_{decay} + L_{mix} \quad (6)$$

5.2.1. Riverine inputs

There are two ^{224}Ra contributions from riverine inputs: dissolved ^{224}Ra in the water and desorbed ^{224}Ra from suspended particles matter (SPM). For the dissolved phase, we determined it by the river freshwater discharge multiply by the river end-member ^{224}Ra activity. In the PRE, the ^{224}Ra activities at O1 ($S = 0.3$) and J1 ($S = 0.1$) station were 87 ± 2.0 and 32 ± 1.1 dpm 100 L^{-1}, which were used as the Pearl River end-members for the dry and wet seasons, respectively. Thus we yielded ^{224}Ra fluxes of $(2.8 \pm 0.1) \times 10^{11}$ and $(2.9 \pm 0.1) \times 10^{11}$ dpm d^{-1} with freshwater discharge of 3.2×10^8 and 9.2×10^8 m^3 d^{-1}, respectively. In the CRE, we used the ^{224}Ra activity at CRE station ($S = 0.1$) as the Changjiang River end-member, thus we yielded ^{224}Ra fluxes of $(2.4 \pm 0.1) \times 10^{11}$ dpm d^{-1} with freshwater discharge of 1.8×10^9 m^3 d^{-1}. Similarly, the term for the desorbed component can be calculated by multiplying the desorbed ^{224}Ra from SPM by the SPM loaded with river. Firstly, we used SPM in the CRE station and employed a repeated leaching method to carry out the laboratory desorption experiment according to our previous work (Gu et al., 2012). Briefly, we used

Table 1
Summary of the parameters used to estimate the flushing time in the PRE.

Parameters	Values		Reference
	Dry season	Wet season	
Surface area, $\times 10^9$ m^2	2	2	Sun et al., 2014
Mean water depth, m	6	6	Sun et al., 2014
River inflow, $\times 10^9$ m^3 d^{-1}	0.32	0.92	This study
Tide range, m	1.2 ± 0.19	1.8 ± 0.42	http://ocean.cnss.com.cn/
Prism, $\times 10^9$ m^3	2.4 ± 0.38	3.6 ± 0.84	This study
Tide period, days	0.52	0.52	Lin and Liang, 1994
Volume, $\times 10^9$ m^3	12	12	This study
b	0.52	0.18	This study
T_f, days	4.8 ± 1.1	1.8 ± 0.6	This study

Ra-free water (after flowing through the Mn-fiber column) to leach a known mass of SPM several times until ^{224}Ra activity in the filtrate no longer increased. Therefore, the exchangeable ^{224}Ra was obtained to be approximately 1.4 dpm g^{-1}. Besides, the SPM loaded by Pear River were 6.5×10^{10} g d^{-1} and 5.0×10^{10} g d^{-1} in the dry and wet season, respectively, and loaded by Changjiang River were 2.0×10^{11} g d^{-1} in the dry season. Consequently, the desorbed ^{224}Ra input by river were estimated to be 9.1×10^{10} dpm d^{-1} in dry season and 7.0×10^{10} dpm d^{-1} in wet season of the PRE, and 2.9×10^{11} dpm d^{-1} in CRE dry season.

5.2.2. Production from the resuspended particles

In an estuary, tidal current and waves are the major drivers for mixing in the water column and they may also scour surficial sediment and resuspended sediment into the water column. Thus, production of desorbable ^{224}Ra from surface-bound ^{228}Th can result in an important inventory, because particle-associated ^{224}Ra would be desorbed in saline water after the particles are resuspended (Beck et al., 2007b). In the PRE, however, the rates of the fluxes from resuspension were not reported in the previous studies. Thus, we use the data from the CRE, estimated by Shen et al. (2008) of 15.7 ± 5.6 mg cm^{-2} d^{-1} as the resuspension rate. Assuming that the ^{224}Ra in the surficial sediment is at a steady state and that tidal currents and waves continuously supply the desorbable ^{224}Ra from the resuspended sediment into the water column, we estimated the ^{224}Ra fluxes desorption from resuspended particles to be $(4.4 \pm 1.6) \times 10^{11}$ dpm d^{-1} both in dry and wet season of the PRE and $(5.5 \pm 3.0) \times 10^{12}$ dpm d^{-1} in the dry season of the CRE.

5.2.3. Diffusion from the bottom sediments

Another significant ^{224}Ra source into the water column of the PRE and CRE is a diffusive flux crossing the sediment-water interface through the sediment pore spaces. Usually, when estimating SGD, the flux of ^{224}Ra diffuses from the sediments can be mediated by only molecular diffusion, and bioirrigation is excluded (Moore, 2010). Therefore, in this study, if we neglected the bioirrigation and followed Hancock et al. (2000), the diffusion rate (F) of ^{224}Ra from the sediment into the water column is expressed as follows:

$$F = -\frac{\phi D_m}{\frac{2\Theta\phi D_m}{-w+\sqrt{w^2+4\Theta\phi D_m\lambda}}}\left(A_w - \frac{\Theta\gamma}{\lambda}\right) \quad (7)$$

By using the definitions and values of these parameters shown in Table 2, the ^{224}Ra diffusion rates from sediment were estimated to be 0.10 and 0.060 dpm cm^{-2} d^{-1} in the PRE for the dry and wet seasons, respectively, and 0.12 dpm cm^{-2} d^{-1} for the CRE, respectively. Similarly, by multiplying the diffusion rates by the surface area of the bottom sediment, the ^{224}Ra fluxes from the sediments diffusions were 2.0×10^{12} and 1.2×10^{12} dpm d^{-1} in the PRE for dry and wet seasons, respectively, and 30×10^{12} dpm d^{-1} for the CRE, respectively. Compared with the long-life Ra isotope (i.e., ^{226}Ra) into the water column from the bottom sediments in the CRE (Gu et al., 2012), the ^{224}Ra flux has a prominent role in the ^{224}Ra mass balance, as well as in the PRE.

5.2.4. Radioactive decay

In the PRE and CRE, the estimated water ages are both on the order of days, the radioactive decay of ^{224}Ra could be an important removal process. Here, we assume a steady state condition during the sampling period, and the flux can be estimated by the decay constant of ^{224}Ra and the ^{224}Ra inventory. Because the pycnocline in the CRE only occurred near the coastal regions which are all in shallow depth (Fig. 4), assuming ^{224}Ra mixed well and distributed uniformly in the vertical profile. Thus the ^{224}Ra inventory can be calculated from the average ^{224}Ra activities multiplied by the volume in the study area of the PRE and CRE. The average ^{224}Ra activities were 190 ± 45.5 and 56 ± 5.0 dpm 100 L^{-1} in the dry and wet seasons in the PRE, respectively, and 34 ± 6.2 dpm 100 L^{-1} in the CRE; these values are assumed to represent the average value in the entire water column. Based on these results, the radioactive decay terms were $(4.3 \pm 1.0) \times 10^{12}$ dpm d^{-1} for the dry season and $(1.3 \pm 0.11) \times 10^{12}$ dpm d^{-1} for the wet season in the PRE and $(55 \pm 10) \times 10^{12}$ dpm d^{-1} in the CRE.

5.2.5. Mixing with seawater

The low ^{224}Ra seawater flows into the PRE and CRE is another significant term for the ^{224}Ra reduction. To estimate the ^{224}Ra fluxes, we used a method based on the inventory of excess ^{224}Ra multiplied by the mixing rate of $1/\tau$ (Kim et al., 2011; Luo et al., 2014). In addition, the excess ^{224}Ra was obtained by the following equation:

$$^{224}Ra_{ex} = {}^{224}Ra_M - f\,{}^{224}Ra_O - (1-f)\,{}^{224}Ra_R \quad (8)$$

where $^{224}Ra_{ex}$ is the excess ^{224}Ra activity, $^{224}Ra_M$ is the measured ^{224}Ra in the PRE and CRE, $^{224}Ra_O$ and $^{224}Ra_R$ are the ^{224}Ra in the open sea water and river water, respectively, and f is the fraction of open sea water. In the PRE, ^{224}Ra activities in the open sea water were 9.2 ± 1.3 (station O5, S = 33.9) and 2.7 ± 0.2 (station J6, S = 32.8) dpm 100 L^{-1} in the dry season and wet season, respectively; the river end-member values are 87 ± 2.0 (station O1, S = 0.3) and 32 ± 1.1 (station J1, S = 0.1) dpm 100 L^{-1} for the dry season and wet season, respectively. Similarity, the ^{224}Ra activities in the open sea water and river water of the CRE were 3.2 ± 0.45 (station A6-11, S = 34.3) and 13 ± 0.69 (station CJR, S = 0.1) dpm 100 L^{-1}, respectively. With these known values, we calculated the excess ^{224}Ra at each station and then the average excess ^{224}Ra were estimated to be 143 ± 45 and 40 ± 7.2 dpm 100 L^{-1} in dry season and wet season in the PRE, respectively, and 30 ± 6.1 dpm 100 L^{-1} in the dry season of the CRE. Therefore, we calculated the ^{224}Ra fluxes from the mixing with open seawater to be $(3.6 \pm 1.4) \times 10^{12}$ dpm d^{-1} and $(2.6 \pm 1.0) \times 10^{12}$ dpm d^{-1} in the PRE for the dry and wet seasons, respectively, and $(22 \pm 7.2) \times 10^{12}$ dpm d^{-1} in the CRE.

5.3. Estimation of SGD into the PRE and CRE

According to Eq. (6), the ^{224}Ra fluxes through SGD are estimated to be $(5.0 \pm 1.7) \times 10^{12}$ dpm d^{-1} (dry season) and $(1.3 \pm 1.0) \times 10^{12}$ dpm d^{-1} (wet season) in the PRE and $(41 \pm 13) \times 10^{12}$ dpm d^{-1} in the CRE. Therefore, we summarized the input and output terms of the ^{224}Ra fluxes in the PRE and CRE (Table 3), suggesting that SGD is the dominate source for ^{224}Ra which accounted for 64% and 33% in the PRE for the dry season and wet season, respectively, and 54% in the CRE.

To quantify the SGD fluxes in the PRE and CRE, the ^{224}Ra end-member values for the potential groundwater seeping into the two estuaries are required. In order not to overestimate SGD flux, we applied the average and maximum activities in groundwater as end-members to estimate SGD fluxes into the PRE and CRE. In this case, we estimated the SGD flux into the PRE at $(4.5–10) \times 10^8$ m^3 d^{-1} and $(1.2–2.7) \times 10^8$ m^3 d^{-1} for the dry season and wet season, respectively, while the SGD flux in the dry season of the CRE was estimated to be $(4.6–11) \times 10^9$ m^3 d^{-1}, which was higher than that calculated in the wet season of $(0.2–1.0) \times 10^9$ m^3 d^{-1} by Gu et al. (2012), showing the same pattern in the PRE; however, some studies reported SGD flux in the wet season was greater (Moore et al., 2006; Garcia-Orellana et al., 2014; Wang et al., 2015). In the PRE, the quantities of the SGD were equivalent to (140–321) % and (13–29) % of the Pearl River water

Table 2
All the definitions and values of these parameters used to calculate the ^{224}Ra diffusion rate from the bottom sediments in the PRE and CRE.

Parameter	Definition	Unit	Value	
			PRE	CRE
Φ	Porosity in the sediment		0.63[a]	0.57[b]
D_m	Molecular diffusion coefficient in the sediment	$cm^2\ d^{-1}$	0.32[b]	0.32[b]
A_w	^{224}Ra activity in the overlying water	$dpm\ cm^{-3}$	0.0019[c](dry), 0.00066[c](wet)	0.00034[c]
w	Sedimentary rate in the sediment	$cm\ d^{-1}$	2.7×10^{-3}[d]	4.1×10^{-3}[e]
Θ	Desorption function for the sediment		0.023[f](dry), 0.0083[f](wet)	0.036[f]
γ	Production rate of the exchangeable ^{224}Ra	$dpm\ cm^{-3}\ d^{-1}$	0.67[g]	0.67[g]
λ	Decay constant of ^{224}Ra	d^{-1}	0.189	0.0189
F	Diffusion rate of ^{224}Ra from the sediment	$dpm\ cm^{-2}\ d^{-1}$	0.10(dry), 0.060(wet)	0.12

[a] Derived from Cai et al. (2015).
[b] Derived from Cai et al.(2014).
[c] We used the average activity in surface water.
[d] Derived from Peng et al. (2007).
[e] Derived from Zhang (2008).
[f] Derived from Gu (2016) of $\Theta = 0.0013 \times S$.
[g] Derived from Hancock et al. (2000).

Table 3
Summary of all the ^{224}Ra terms in the PRE and CRE.

Term	^{224}Ra flux ($\times 10^{12}$ dpm d^{-1})		
	Dry season in PRE	Wet season in PRE	Dry season in CRE
Fluxes OUT			
Decay	4.3 ± 1.0	1.3 ± 0.11	55 ± 10
Mixing with the open sea	3.6 ± 1.4	2.6 ± 1.0	22 ± 7.2
Fluxes IN			
River	0.37 ± 0.010	1.0 ± 0.010	0.53 ± 0.010
Desorption from the resuspended particles	0.44 ± 0.16	0.44 ± 0.16	5.5 ± 2.0
Diffusion from the sediments	2.0	1.2	30
SGD	5.0 ± 1.7	1.3 ± 1.0	41 ± 13

runoff in the dry season (river discharge of $3.2 \times 10^8\ m^3\ d^{-1}$) and wet season (river discharge of $9.2 \times 10^8\ m^3\ d^{-1}$), respectively, and in the CRE, the SGD flux achieved (256–622) % of the Changjiang River discharge ($1.8 \times 10^9\ m^3\ d^{-1}$) in the dry season.

Next, we estimated the uncertainties in the calculation of the SGD-derived ^{224}Ra and SGD flux, which were based on the ^{224}Ra measurement error and error propagation rules. As presented in the ^{224}Ra mass balance model (Eq. (6)), the estimations of SGD could be influenced by a number of factors. In the PRE and CRE, the most significant terms in the ^{224}Ra balance are decay, mixing with open sea and diffusion from sediments, so these terms may mainly contribute to the uncertainties estimations. The errors of ^{224}Ra decay loss are estimated from the uncertainties of observed ^{224}Ra inventories, which led to SGD fluxes errors to be 8.9–20% in the PRE, and 24% in the CRE, respectively. For the mixing term, in the PRE the uncertainties are highly sensitive to the water age, which an error of 1 day could cause a change of 12–72% in the SGD flux, while only change of 4.2% in the CRE. Given that the half-life of ^{224}Ra is short, the uncertainties of diffusion from the bottom sediments should be considered in the SGD flux estimation, and it was noted that a 10% change in the ^{224}Ra of the sediments diffusion inputs can change the SGD flux by 4.0% in the PRE and 7.2% in the CRE, respectively. In addition, the ^{224}Ra activity in groundwater is also a significant factor that can influence the uncertainty in the SGD flux. Because of the possible different stratigraphy and geological in the coastal aquifers of the PRE and CRE, ^{224}Ra activities in groundwater were in wide range. In order to obtain the representative SGD estimations, we used an overall range to represent the SGD flux rather than single ^{224}Ra activity in groundwater for estimation.

In the PRE and CRE, the fresh groundwater recharge rate into our study areas along the shoreline are $4.3 \times 10^6\ m^3\ d^{-1}$ and $49 \times 10^6\ m^3\ d^{-1}$, respectively (Du, 2006; Zhu et al., 2004), which are only 0.41–3.7% and 0.44–1.1% of our estimated SGD fluxes, suggesting that almost all of the SGD in the two estuaries derived from the recirculated groundwater. In addition, the higher estimated SGD fluxes coincided with lower precipitation and higher salinity in both the PRE and CRE due to seawater intrusion (Fig. 6), which also indicated that the recirculated groundwater dominated the total SGD in this study. Usually, the recirculated groundwater is mainly caused by the tide; however, the tide heights throughout the sampling periods are 1.7 m and 2.6 m in the PRE and CRE, respectively, which are both similar in the dry and wet seasons. Therefore, we thought that there must be other factors that drive the higher SGD flux in the dry season. In such river-dominated estuaries, these factors may be seawater intrusion or high sea level (Gonneea et al., 2013). In the dry season, the water age is higher than that in wet season, which may extend the residence time of higher salinity water in the estuary, thus driving more recirculated groundwater.

5.4. Evaluation of the SGD-derived nutrient fluxes into the PRE and CRE

Except to be an important part of the assessment of water budgets, nutrient transport through SGD has been shown to be a significant component of nutrient budgets in the estuaries (e.g., Lee et al., 2009; Rengarajan and Sarma, 2015). The nutrient concentrations ($\mu mol\ L^{-1}$) in groundwater of the PRE ranged from 23 to 1581, with an average of 412 for DIN, from 0.14 to 28.5, with an average of 7.8 $\mu mol\ L^{-1}$ for PO_4^{3-} and from 12 to 666, with an average of 238 for $Si(OH)_4$. While in groundwater of the CRE, DIN concentrations ranged from 81 to 489 $\mu mol\ L^{-1}$, with an average of 271 $\mu mol\ L^{-1}$, PO_4^{3-} concentrations ranged from 1.5 to 5.4 $\mu mol\ L^{-1}$, with an average of 3.0 $\mu mol\ L^{-1}$ and $Si(OH)_4$ concentrations ranged

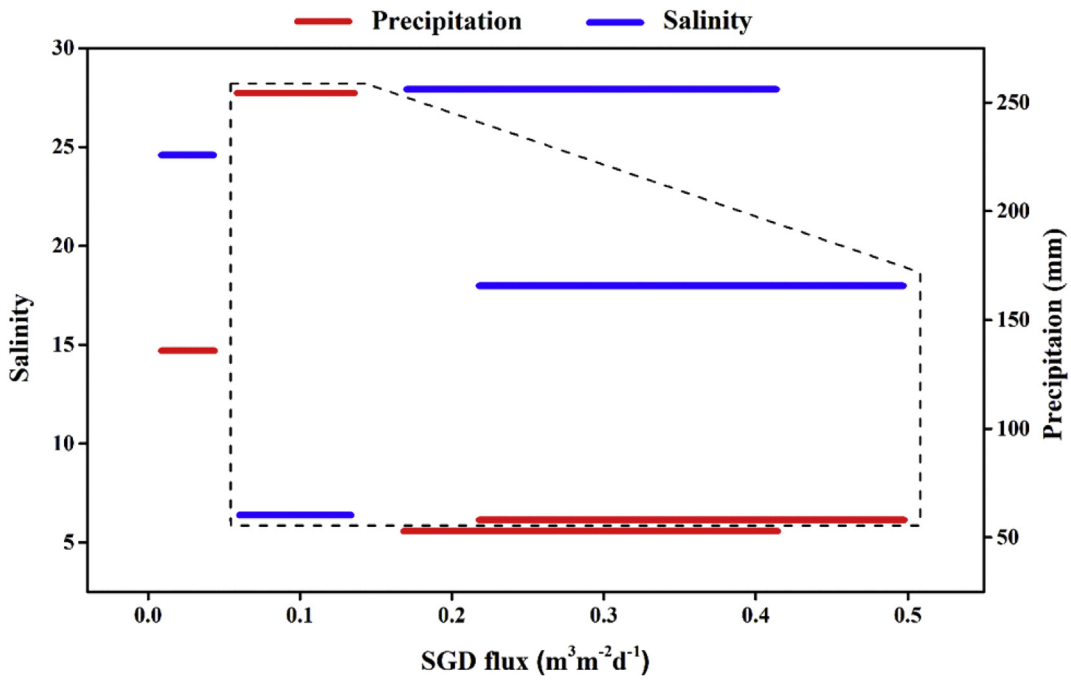

Fig. 6. The relationship between SGD rate ranges and salinity, precipitation in the PRE and CRE. The dashed line represent the SGD flux in the PRE (color figure online).

from 64 to 486 μmol L^{-1}, with an average of 230 μmol L^{-1} (Supplementary Table). We can see that both in the PRE and CRE nutrient concentrations existed large spatial variations in groundwater. Unlike the SGD flux estimation, here we used the average and minimum nutrient concentrations in groundwater as end-members to estimate the SGD-derived nutrient fluxes (Liu et al., 2012). Assuming the nutrient concentrations in groundwater are the same for both seasons, the SGD-derived nutrient loads (mol d^{-1}) during the dry and wet seasons in the PRE were estimated to be $(1.0–43)\times10^7$ for DIN, $(0.62–81)\times10^5$ for PO_4^{3-}, and $(0.52–25)\times10^7$ for $Si(OH)_4$ and $(0.26–11)\times10^7$ for DIN, $(0.16–21)\times10^5$ for PO_4^{3-}, and $(0.14–6.4)\times10^7$ for $Si(OH)_4$, respectively. Similarly, the nutrient fluxes (mol d^{-1}) via the SGD in the CRE were $(3.7–30)\times10^8$ for DIN, $(6.7–34)\times10^6$ for PO_4^{3-}, $(2.9–26)\times10^9$ for $Si(OH)_4$ in the dry season and $(0.16–3.0)\times10^8$ for DIN, $(0.30–3.3)\times10^6$ for PO_4^{3-}, $(0.13–2.5)\times10^8$ for $Si(OH)_4$ in the wet season. It was clearly observed that the SGD-derived nutrient fluxes in the dry season were much higher than those in the wet season in both PRE and CRE.

Fig. 7 demonstrates the nutrient fluxes through SGD into the PRE and CRE as contrasted with the riverine nutrient fluxes which were determined by multiplying the average discharge of the Pear River and Changjiang River by the average nutrient concentrations in each river water end-member. We noticed that the SGD represented a substantial contribution to the nutrient loading to the PRE, and the SGD-derived DIN, PO_4^{3-} and $Si(OH)_4$ were even 5 times the riverine inputs in the dry season. During the wet season, the DIN, PO_4^{3-} and $Si(OH)_4$ contributed from SGD were approximately 1.5–60%, 1.1–150%, and 0.78–37%, respectively. The DIN and PO_4^{3-} in the wet season were comparable with fractions observed in the Pearl River for the same season (Liu et al., 2012). In addition, in the CRE, the nutrient derived by SGD were more than 2–12 times that of the Changjiang River inputs.

In general, N: P ratios in groundwater are much higher than the Redfield N: P ratios of 16:1. In this study, the SGD-derived N: P ratios in the PRE and CRE were approximately 53 and 90, respectively, which were higher than the Redfield ratio, but they were not significantly different from the values found in the river water (Fig. 7). The groundwater, except for supplying the high DIN and PO_4^{3-} fluxes into the PRE and CRE, also modifies the N: P ratios, which may have a significant impact on the ecosystem structure and phytoplankton composition and then may lead to eutrophication/red tides (Anderson, 1989). During red tides break, *Skeletonema* spp. are generally considered to be the dominant phytoplankton population in the PRE and CRE (Jiang et al., 2014; Liu et al., 2013). The PO_4^{3-} concentration is considered as the limiting factor for the *Skeletonema* spp. outbreaks and the nutrient supporting the red tides bloom (e.g., Hong et al., 1993; Wang, 2001). Therefore, nutrient fluxes with high N: P ratios by SGD into the PRE and CRE could affect the ecology of coastal waters by forcing a primary production change or exacerbating towards P-limitation. As one of the important substance pathway, basically, SGD is ubiquitous along the coasts. Although SGD is not a new nutrient source, it may deliver more concentrated substance with the rapid economic development and population growth along coasts of the PRE and CRE in past several decades, which may lead to excessive release of waste into the estuaries. Therefore, the SGD-derived substance, especially nutrient, should have an influence on the ecosystem which could result in some environment problems and should be paid more attention.

6. Summary

In the present study we estimated SGD fluxes into two major and river-dominated estuaries of China: the Pearl River Estuary (PRE) and the Changjiang River Estuary (CRE). Based on the ^{224}Ra spatial and temporal distributions in the PRE and CRE conducted in 2014 and 2015, we draw the following preliminary conclusions.

1) It is quite necessary to employ the appropriate method to estimate water age in different types of estuaries. The average water ages in the PRE were estimated to be 4.8 ± 1.1 days and 1.8 ± 0.6 days in the dry season and wet season, respectively, and 11.7 ± 5.0 days in the dry season of the CRE.

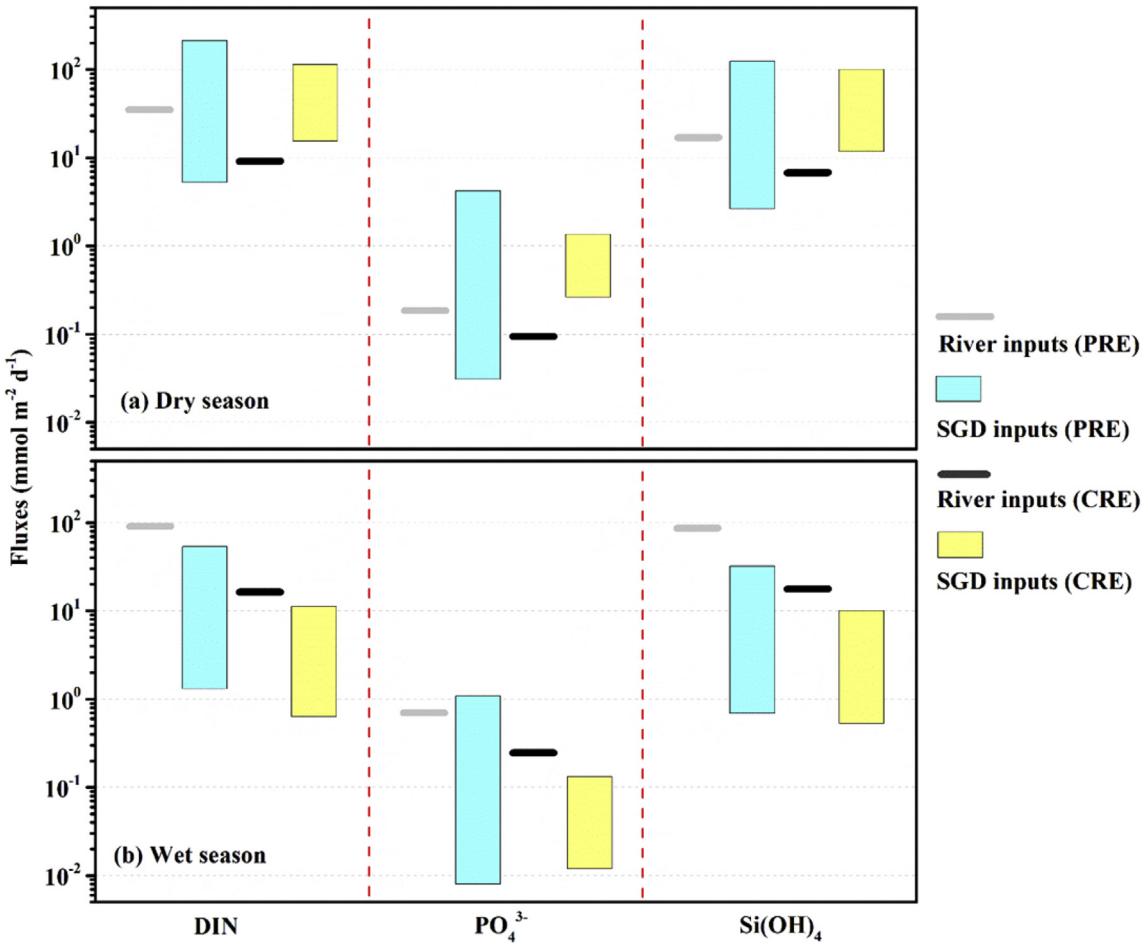

Fig. 7. Comparison of SGD and river-derived nutrient fluxes in the dry (a) and wet (b) season in the PRE and CRE. The SGD flux in the wet season of the CRE was derived from Gu et al. (2012), and nutrient concentrations in the Changjiang River were derived from Wang et al. (2013).

2) By utilizing a ^{224}Ra mass balance model, the SGD fluxes rivals the rivers discharge into each of the two estuaries in the dry season, which reached as high as (140–321) % and (256–622) % in the PRE and CRE, respectively. In the wet season of the PRE, the SGD flux was approximately (13–29) % of the runoff the Pearl River;
3) The SGD-derived nutrient loading appeared to be a major source of nutrient input into the PRE and CRE, especially in the dry season with more recirculated seawater intrusion. The nutrient-enriched SGD with high N: P ratios may lead to more frequently occurring eutrophication and red tides in the PRE and CRE.

Acknowledgements

The data reported in this paper were provide by the State Key Laboratory of Estuarine and Coastal Research, East China Normal University. This work was supported by the Key Project of Chinese National Programs for Fundamental Research and Development (973 Program) (grant number 2014CB441502), the National Science Fund of China (grant number 41376089, 41376086), the Program of the State Key Laboratory of Estuarine and Coastal Research (SKLEC-2017RCDW01) and the Programme of Introducing Talents of Discipline to Universities (111 project, grant number B08022).

Appendix A. Supplementary data

Supplementary data related to this article can be found at https://doi.org/10.1016/j.ecss.2018.02.005.

References

Anderson, D.M., 1989. Toxic algal blooms and red tides: a global prespective. Red Tides: Biol. Environ. Sci. Toxicol. 11–16.
Beck, A.J., Tsukamoto, Y., Tovar-Sanchez, A., Huerta-Diaz, M., Bokuniewicz, H.J., Sanudo-Wilhelmy, S.A., 2007a. Importance of geochemical transformations in determining submarine groundwater discharge-derived trace metal and nutrient fluxes. Appl. Geochem. 22, 477–490. https://doi.org/10.1016/j.apgeochem.2006.10.005.
Beck, A.J., Rapaglia, J.P., Cochran, J.K., Bokuniewicz, H.J., 2007b. Radium mass-balance in Jamaica Bay, NY: evidence for a substantial flux of submarine groundwater. Mar. Chem. 106, 419–441. https://doi.org/10.1016/j.marchem.2007.03.008.
Burnett, W.C., Bokuniewicz, H., Huettel, M., Moore, W.S., Taniguchi, M., 2003. Groundwater and pore water inputs to the coastal zone. Biogeochemistry 66, 3–33. https://doi.org/10.1023/B:BIOG.0000006066.21240.53.
Charette, M.A., Moore, W.S., Burnett, W.C., 2008. Uranium-and thorium-series nuclides as tracers of submarine groundwater discharge. Radioact. Environ. 13, 155–191. https://doi.org/10.1016/S1569-4860(07)00005-8.
China hydrological geological map, 1984. China Cartographic Publishing House, Prepared by the Institute of Hydrogeology and Environmental Geology. Chinese Academy of Geological Sciences.
Cai, W.J., Dai, M., Wang, Y., Zhai, W., Huang, T., Chen, S., Zhang, F., Chen, Z., Wang, Z., 2004. The biogeochemistry of inorganic carbon and nutrients in the Pearl River estuary and the adjacent Northern South China Sea. Cont. Shelf Res. 24, 1301–1319. https://doi.org/10.1016/j.csr.2004.04.005.
Cai, P., Shi, X., Moore, W.S., Peng, S., Wang, G., Dai, M., 2014. ^{224}Ra:^{228}Th disequilibrium in coastal sediments: implications for solute transfer across the sediment-water interface. Geochim. Cosmochim. Acta 125, 68–84. https://doi.org/10.1016/j.gca.2013.09.029.
Cai, P., Shi, X., Hong, Q., Li, Q., Liu, L., Guo, X., Dai, M., 2015. Using ^{224}Ra/^{228}Th disequilibrium to quantify benthic fluxes of dissolved inorganic carbon and

nutrients into the Pearl River Estuary. Geochim. Cosmochim. Acta 170, 188–203. https://doi.org/10.1016/j.gca.2015.08.015.
Chen, X., Zhu, L., Zhang, H., 2007. Numerical simulation of summer circulation in the East China Sea and its application in estimating the sources of red tides in the Yangtze River estuary and adjacent sea areas. J. Hydrodyn. Ser. B 19, 272–281. https://doi.org/10.1016/S1001-6058(07)60059-6.
Dai, S.B., Lu, X.X., 2014. Sediment load change in the yangtze river (Changjiang): a review. Geomorphology 215, 60–73. https://doi.org/10.1016/j.geomorph.2013.05.027.
Du, Q.T., 2006. The environmental and safety problems in exploiting and utilizing groundwater resources in the Pearl River delta regions. Guangdong Geol. 21, 29–31 (in Chinese with English abstract).
Garcia-Orellana, J., Rodellas, V., Casacuberta, N., Lopez-Castillo, E., Vilarrasa, M., Moreno, V., Garcia-Solsona, E., Masqué, P., 2013. Submarine groundwater discharge: natural radioactivity accumulation in a wetland ecosystem. Mar. Chem. 156, 61–72. https://doi.org/10.1016/j.marchem.2013.02.004.
Garcia-Orellana, J., Cochran, J.K., Boluniewicz, H., Daniel, J.W.R., Rodellas, V., Heilbrun, C., 2014. Evaluation of ^{224}Ra as a tracer for submarine groundwater discharge in Long Island Sound (NY). Geochim. Cosmochim. Acta 141, 314–330. https://doi.org/10.1016/j.gca.2014.05.009.
Garcia-Solsona, E., Garcia-Orellana, J., Masqué, P., Dulaiova, H., 2008. Uncertainties associated with ^{223}Ra and ^{224}Ra measurements in water via a delayed coincidence counter (RaDeCC). Mar. Chem. 109, 198–219. https://doi.org/10.1016/j.marchem.2007.11.006.
Gonneea, M.E., Mulligan, A.E., Charette, M.A., 2013. Climate-driven sea level anomalies modulate coastal groundwater dynamics and discharge. Geophys. Res. Lett. 40 (11), 2701–2706. https://doi.org/10.1002/grl.50192.
Gu, H., 2016. A Quantitative Study on the Sources and Sinks of Radium Isotopes in Near-shore Waters. Ph. D. Thesis. East China Normal Univ, Shanghai, China (unpublished).
Gu, H., Moore, W.S., Zhang, L., Du, J., Zhang, J., 2012. Using radium isotopes to estimate the residence time and the contribution of submarine groundwater discharge (SGD) in the Changjiang effluent plume. East China Sea. Cont. Shelf Res. 35, 95–107. https://doi.org/10.1016/j.csr.2012.01.002.
Hancock, G.J., Webster, I.T., Ford, P.W., Moore, W.S., 2000. Using Ra isotopes to examine transport processes controlling benthic fluxes into a shallow estuarine lagoon. Geochim. Cosmochim. Acta 64, 3685–3699. https://doi.org/10.1016/S0016-7037(00)00469-5.
Harrison, P.J., Yin, K., Lee, J.H.W., Gan, J., Liu, H., 2008. Physical-biological coupling in the Pearl River estuary. Cont. Shelf Res. 28, 1405–1415. https://doi.org/10.1016/j.csr.2007.02.011.
He, B., Dai, M., Zhai, W., Wang, L., Wang, K., Chen, J., Lin, J., Han, A., Xu, Y., 2010. Distribution, degradation and dynamics of dissolved organic carbon and its major compound classes in the Pearl River estuary, China. Mar. Chem. 119, 52–64. https://doi.org/10.1016/j.marchem.2009.12.006.
Hong, J.C., Huang, X.Q., Jiang, X.S., Wang, G.L., 1993. Analysis on the caused factors for the Skeletonema costatum red tide in Shengshan waters. Acta Oceanol. Sinica 15, 135–141 (in Chinese with English abstract).
Huang, X.P., Huang, L.M., Yue, W.Z., 2003. The characteristics of nutrients and eutrophication in the Pearl River estuary, South China. Mar. Pollut. Bull. 47, 30–36. https://doi.org/10.1016/S0025-326X(02)00474-5.
Hwang, D., Kim, G., Lee, Y., Yang, H., 2005b. Estimating submarine inputs of groundwater and nutrients to a coastal bay using radium isotopes. Mar. Chem. 96 (1), 61–71. https://doi.org/10.1016/j.marchem.2004.11.002.
Hwang, D., Lee, Y., Kim, G., 2005a. Large submarine groundwater discharge and benthic eutrophication in Bangdu Bay on volcanic Jeju Island, Korea. Limnol. Oceanogr. 50, 1393–1403. https://doi.org/10.4319/lo.2005.50.5.1393.
Jiang, Z., Liu, J., Chen, J., Chen, Q., Yan, X., Xuan, J., Zeng, J., 2014. Responses of summer phytoplankton community to drastic environmental changes in the Changjiang (Yangtze River) estuary during the past 50 years. Water Res. 54, 1–11. https://doi.org/10.1016/j.watres.2014.01.032.
Jing, J., Sun, J., Han, S., Huang, G., Chen, X., Zhang, Y., Liu, J., 2010. Distribution of acid and acidified groundwater in Pearl River deltas. Shanghai Geol. 2, 8–12 (in Chinese with English abstract).
Kim, G., Kim, J., Hwang, D., 2011. Submarine groundwater discharge from oceanic islands standing in oligotrophic oceans: implications for global biological production and organic carbon fluxes. Limnol. Oceanogr. 56, 673–682. https://doi.org/10.4319/lo.2011.56.2.0673.
Kolker, A.S., Cable, J.E., Johannesson, K.H., Allison, M.A., Inniss, L.V., 2013. Pathways and processes associated with the transport of groundwater in deltaic systems. J. Hydrol 498, 319–334. https://doi.org/10.1016/j.jhydrol.2013.06.014.
Lee, Y., Hwang, D., Kim, G., Lee, W., Oh, H., 2009. Nutrient inputs from submarine groundwater discharge (SGD) in Masan Bay, an embayment surrounded by heavily industrialized cities, Korea. Sci. Total Environ. 407, 3181–3188. https://doi.org/10.1016/j.scitotenv.2008.04.013.
Li, M., Xu, K., Watanabe, M., Chen, Z., 2007. Long-term variations in dissolved silicate, nitrogen, and phosphorus flux from the Yangtze River into the East China Sea and impacts on estuarine ecosystem. Estuar. Coast Shelf Sci. 71, 3–12. https://doi.org/10.1016/j.ecss.2006.08.013.
Lin, Z., Liang, S., 1994. A Study on the tidal current in the waters of the Pearl River mouth. Mar. Sci. Bull. 15, 11–22 (in Chinese with English abstract).
Liu, L., Zhou, J., Zheng, B., Cai, W., Lin, K., Tang, J., 2013. Temporal and spatial distribution of red tide outbreaks in the Yangtze River Estuary and adjacent waters, China. Mar. Pollut. Bull. 72, 213–221. https://doi.org/10.1016/j.marpolbul.2013.04.002.
Liu, Q., Dai, M., Chen, W., Huh, C.-A., Li, Q., Charette, M.A., 2012. How significant is submarine groundwater discharge and its associated dissolved inorganic carbon in a river-dominated shelf system? Biogeosciences 9, 1777–1795. https://doi.org/10.5194/bgd-8-12381-2011.
Liu, Q., Charette, M.A., Henderson, P.B., McCorkle, D.C., Martin, W., Dai, M., 2014. Effect of submarine groundwater discharge on the coastal ocean inorganic carbon cycle. Limnol. Oceanogr. 59, 1529–1554. https://doi.org/10.4319/lo.2014.59.5.1529.
Liu, S.M., Zhang, J., Chen, H.T., Zhang, G.S., 2005. Factors influencing nutrient dynamics in the eutrophic Jiaozhou Bay, North China. Prog. Oceanogr. 66, 66–85. https://doi.org/10.1016/j.pocean.2005.03.009.
Liu, S.M., Qi, X.H., Li, X., Ye, H.R., Wu, Y., Ren, J.L., Zhang, J., Xu, W.Y., 2016. Nutrient dynamics from the Changjiang (yangtze river) estuary to the east China sea. J. Marine Syst. 154, 15–27. https://doi.org/10.1016/j.jmarsys.2015.05.010.
Lu, Z., Gan, J., 2015. Controls of seasonal variability of phytoplankton blooms in the Pearl River Estuary. Deep-Sea Res. Pt. II. 117, 86–96. https://doi.org/10.1016/j.dsr2.2013.12.011.
Luo, X., Jiao, J.J., Moore, W.S., Lee, C.M., 2014. Submarine groundwater discharge estimation in an urbanized embayment in Hong Kong via short-lived radium isotopes and its implication of nutrient loadings and primary production. Mar. Pollut. Bull. 82 (1), 144–154. https://doi.org/10.1016/j.marpolbul.2014.03.005.
Mao, Q., Shi, P., Yin, K., Gan, J., Qi, Y., 2004. Tides and tidal currents in the Pearl River Estuary. Coast. Shelf Sci. 24, 1797–1808. https://doi.org/10.1016/j.csr.2004.06.008.
McCoy, C., Viso, R., Peterson, R.N., Libes, S., Lewis, B., Ledoux, J., Voulgaris, G., Smith, E., Sanger, D., 2011. Radon as an indicator of limited cross-shelf mixing of submarine groundwater discharge along an open ocean beach in the South Atlantic Bight during observed hypoxia. Cont. Shelf Res. 31, 1306–1317. https://doi.org/10.1016/j.csr.2011.05.009.
Moore, W.S., 1976. Sampling ^{288}Ra in the deep ocean. Deep Sea Res. Oceanogr. Abstr. 23, 647–651. https://doi.org/10.1016/0146-6291(77)90131-x.
Moore, W.S., 1996. Large groundwater inputs to coastal waters revealed by ^{226}Ra enrichments. Nature 380, 612–614. https://doi.org/10.1038/380612a0.
Moore, W.S., 2000. Ages of continental shelf waters determined from ^{223}Ra and ^{224}Ra. J. Geophys. Res. 105, 22117–22122. https://doi.org/10.1029/1999jc000289.
Moore, W.S., 2003. Sources and fluxes of submarine groundwater discharge delineated by radium isotopes. Biogeochemistry 66, 75–93. https://doi.org/10.1023/b:biog.0000006065.77764.a0.
Moore, W.S., 2010. The effect of submarine groundwater discharge on the ocean. Ann. Rev. Mar. Sci. 2, 59–88. https://doi.org/10.1146/annurev-marine-120308-081019.
Moore, W.S., Arnold, R., 1996. Measurement of ^{223}Ra and ^{224}Ra in coastal waters using a delayed coincidence counter. J. Geophys. Res.: Oceans 101, 1321–1329. https://doi.org/10.1029/95jc03139.
Moore, W.S., Blanton, J.O., Joye, S.B., 2006. Estimates of flushing times, submarine groundwater discharge, and nutrient fluxes to Okatee Estuary, South Carolina. J. Geophys. Res. 111. https://doi.org/10.1029/2005jc003041.
Moore, W.S., Krest, J., 2004. Distribution of ^{223}Ra and ^{224}Ra in the plumes of the Mississippi and atchafalaya rivers and the gulf of Mexico. Mar. Chem. 86, 105–119. https://doi.org/10.1016/j.marchem.2003.10.001.
Moore, W.S., Sarmiento, J.L., Key, R.M., 2008. Submarine groundwater discharge revealed by ^{228}Ra distribution in the upper Atlantic Ocean. Nat. Geosci. 1, 309–311. https://doi.org/10.1038/ngeo183.
Peng, X., Wang, Z., Mai, B., Chen, F., Chen, S., Tan, J., Yu, Y., Tang, C., Li, K., Zhang, G., Yang, C., 2007. Temporal trends of nonylphenol and bisphenol A contamination in the Pearl River Estuary and the adjacent South China Sea recorded by dated sedimentary cores. Sci. Total Environ. 384, 393–400. https://doi.org/10.1016/j.scitotenv.2007.05.043.
Rengarajan, R., Sarma, V.V.S.S., 2015. Submarine groundwater discharge and nutrient addition to the coastal zone of the Godavari estuary. Mar. Chem. 172, 57–69. https://doi.org/10.1016/j.marchem.2015.03.008.
Sanford, L.P., Boicourt, W.C., Rives, S.R., 1992. 1992. Model for estimating tidal flushing of small embayments. J. Waterw., Port, Coastal, Ocean Eng 118, 635–654. https://doi.org/10.1061/(ASCE)0733-950X, 118:6(635).
Shen, Z., Zhou, S., Pei, S., 2008. Transfer and transport of phosphorus and silica in the turbidity maximum zone of the Changjiang estuary. Estuar. Coast Shelf Sci. 78, 481–492. https://doi.org/10.1016/j.ecss.2008.01.010.
Stewart, B.T., Santos, I.R., Tait, D.R., Macklin, P.A., Maher, D.T., 2015. Submarine groundwater discharge and associated fluxes of alkalinity and dissolved carbon into Moreton Bay (Australia) estimated via radium isotopes. Mar. Chem. 174, 1–12. https://doi.org/10.1016/j.marchem.2015.03.019.
Sun, J., Lin, B., Li, K., Jiang, G., 2014. A modelling study of residence time and exposure time in the Pearl River Estuary, China. J. Hydro-Environ Res. 8, 281–291. https://doi.org/10.1016/j.jher.2013.06.003.
Wang, J., 2001. Algea bloom monitor in zhoushan archipelago sea area. J. Zhejiang Ocean Univ., Nat. Sci. 20, 62–65.
Wang, K., Chen, J., Jin, H., Li, H., Gao, H., Lu, Y., Xu, J., Weng, H., 2013. Nutrient structure and relative potential limitation in Changjiang River estuary and adjacent east China sea. Acta Oceanol. Sinica 35, 128–136 (in Chinese with English abstract). https://doi.org/10.3969/j.issn.0253-4193.2013.03.015.
Wang, Y., Jiao, J.J., 2012. Origin of groundwater salinity and hydrogeochemical processes in the confined Quaternary aquifer of the Pearl River Delta, China. J. Hydrol. 438, 112–124. https://doi.org/10.1016/j.jhydrol.2012.03.008.
Wang, G., Wang, Z., Zhai, W., Moore, W.S., Li, Q., Yan, X., Qi, D., Jiang, Y., 2015. Net

subterranean estuarine export fluxes of dissolved inorganic C, N, P, Si, and total alkalinity into the Jiulong River estuary, China. Geochim. Cosmochim. Acta 149, 103–114. https://doi.org/10.1016/j.gca.2014.11.001.

Xu, B., Dimova, N.T., Zhao, L., Jiang, X., Yu, Z., 2013. Determination of water ages and flushing rates using short-lived radium isotopes in large estuarine system, the Yangtze River Estuary. China. Estuar. Coast. Shelf Sci. 121–122, 61–68. https://doi.org/10.1016/j.ecss.2013.02.005.

Yan, H., Dai, Z., Li, J., Zhao, J., Zhang, X., Zhao, J., 2011. Distributions of sediments of the tidal flats in response to dynamic actions, Yangtze (Changjiang) Estuary. J. Geogr. Sci. 21, 719–732. https://doi.org/10.1007/s11442-011-0875-0.

Zhang, J., 2008. The Comparison Study on the Sedimentation Rate of the Changjiang Estuary and its Adjacent Area. M.S. Thesis. East China Normal Univ, Shanghai, China (unpublished).

Zhang, J., Zhang, Z.F., Liu, S.M., Wu, Y., Xiong, H., Chen, H.T., 1999. Human impacts on the large world rivers: would the Changjiang (Yangtze River) be an illustration? Global Biogeochem. Cycles 13, 1099–1105. https://doi.org/10.1029/1999gb900044.

Zhang, W., Zheng, J., Xiaomei, J., Hoitink, A.J.F., Van Der Vegt, M., Zhu, Y., 2013. Surficial sediment distribution and the associated net sediment transport pattern in the Pearl River Estuary, South China. Cont. Shelf Res. 61, 41–51. https://doi.org/10.1016/j.csr.2013.04.011.

Zhu, D.K., Wang, Y., Wang, D., Wang, L.C., 2004. Study of water environment and water resources on the delta plain of the Changjiang River. Quat. Sci. 24, 486–494 (in Chinese with English abstract).